

## **TURBULENT MIXED CONVECTION WITHIN RAPIDLY ROTATING HEATED ANNULAR CAVITIES WITH AN AXIAL THROUGHFLOW**

**E.M. Smirnov, S.I. Smirnov, A.G. Abramov, S.A. Galaev**

Peter the Great St. Petersburg Polytechnic University,  
St. Petersburg, Russian Federation

The results of eddy-resolving numerical simulation of a turbulent mixed convection in a system of three identical, rapidly rotating annular cavities are presented. The cavities are heated from the side of the disk surfaces and from the periphery (the same distribution of the surface temperature is set for all the cavities), and heat removal proceeds by an axial air throughflow in the narrow channel, annular within the cavity system. The computations based on the Implicit LES method have been carried out in view of the conditions close to the experiments known from the literature for a single cavity; the rotational Reynolds number was 200,000, the grid dimension was 17 million cells. The complex multiscale flow structure and the influence of the input aerodynamic and thermal conditions, which are not identical for the cavities included in the system, on the local heat transfer from disk surfaces are discussed.

**Keywords:** mixed convection, rapidly rotating annular cavity, axial throughflow, global circulation

**Citation:** Smirnov E.M., Smirnov S.I., Abramov A.G., Galaev S.A., Turbulent mixed convection within rapidly rotating heated annular cavities with an axial throughflow, St. Petersburg Polytechnical State University Journal. Physics and Mathematics. 14 (3) (2021) 21–34. DOI: 10.18721/JPM.14302

This is an open access article under the CC BY-NC 4.0 license (<https://creativecommons.org/licenses/by-nc/4.0/>)

## **ТУРБУЛЕНТНАЯ СМЕШАННАЯ КОНВЕКЦИЯ В БЫСТРОВРАЩАЮЩИХСЯ ОБОГРЕВАЕМЫХ КОЛЬЦЕВЫХ ПОЛОСТЯХ ПРИ ПРОХОЖДЕНИИ ЧЕРЕЗ НИХ ОСЕВОГО ПОТОКА**

**Е.М. Смирнов, С.И. Смирнов, А.Г. Абрамов, С.А. Галаев**

Санкт-Петербургский политехнический университет Петра Великого,  
Санкт-Петербург, Российская Федерация

Представлены результаты вихреразрешающего численного моделирования турбулентной смешанной конвекции в системе из трех одинаковых, быстро вращающихся кольцевых полостей. Полости обогреваются со стороны дисковых поверхностей и с периферии (для всех полостей задано одно и то же распределение поверхностной температуры), а теплоотвод осуществляется транзитным осевым потоком воздуха, протекающим по узкому (в пределах системы полостей) кольцевому каналу. Расчеты на основе метода Implicit LES проведены с учетом условий эксперимента, известных из литературы. Вращательное число Рейнольдса составляло 200 тыс., размерность сетки — 17 млн. ячеек. Обсуждается сложная многомасштабная структура течения и влияние на локальную теплоотдачу с дисковых поверхностей входных аэродинамических и тепловых условий, не являющихся идентичными для включенных в систему полостей.

**Ключевые слова:** смешанная конвекция, быстро вращающаяся кольцевая полость, транзитный осевой поток, глобальная циркуляция

**Ссылка при цитировании:** Смирнов Е.М., Смирнов С.И., Абрамов А.Г., Галаев С.А. Турбулентная смешанная конвекция в быстро вращающихся обогреваемых кольцевых полостях при прохождении через них осевого потока // Научно-технические ведомости СПбГПУ. Физико-математические науки. 2021. Т. 14. № 3. С. 21–34. DOI: 10.18721/JPM.14302

## Introduction

While gaining a deep and reliable understanding of the mechanisms behind local heat transfer in rapidly rotating annular cavities heated from disk surfaces under axial throughflow of cooling gas is important on its own, it is also crucial in the field of turbomachinery, where such configurations are widely used for cooling rotors of axial compressors in gas turbine engines [1 – 4].

Because disk surfaces bounding the cavities are opaque and rotating rapidly, it is difficult to obtain reliable quantitative experimental data characterizing the convection that develops in these cavities, and unsteady local heat transfer. Experimental studies are typically limited to visual observations and measurements of local and integral heat transfer, averaged over time [1 – 3, 5, 6].

Much hope is therefore pinned on modern methods of computational fluid dynamics and heat transfer, as well as supercomputer technologies that allow high-precision eddy-resolving simulation. Direct numerical simulation (DNS) and the implicit large eddy simulation (LES), i.e., ILES, where the role of small-scale physical dissipation is replaced by dissipative properties of the numerical scheme, seem to show the greatest promise.

The initial experience of using the ILES method is described in [7 – 10]. The corresponding computations were carried out on grids with moderate dimensions (up to 100,000 cells) and did not yield an acceptable agreement with the experimental data for local heat transfer on disks, which was attributed to inaccurate modeling of turbulent flow in the zone where axial flow mixes with the gas circulating in the cavity.

The characteristic features of the flow structure known from the literature were successfully reproduced by computations of turbulent mixed convection in a single rapidly rotating ventilated annular cavity heated from the disks [11 – 13], carried out recently by the ILES and RANS/ILES methods (Reynolds-averaged Navier – Stokes equations) using grids with dimensions of up to several million cells. However, this left open the question about the reasons for the constant discrepancy between the simulation results and experimental data on heat transfer from disk surfaces.

Notably, it is difficult to fully reproduce the experimental conditions in the computations due to uncertainties in imposing boundary conditions. In particular, this refers to aerodynamic and thermal conditions at the inlet to the cavity: an unperturbed uniform velocity profile and a constant temperature in the inlet section of the channel supplying the coolant are generally imposed in the computations performed for a single cavity; however, the flow at the inlet to the cavity is non-uniform and turbulent in the experiments.

In view of the above, it seems particularly interesting to conduct numerical studies of mixed convection in a system of sequentially located cavities, when the experimental conditions can be simulated more accurately, which, together with detailed resolution of processes (that are significant for the problem) on refined grids, allows expecting better agreement with the measurement data. Multistage cavities are becoming the focus of increased attention in experimental studies; for example, measurements of the time-averaged temperature and local heat transfer on disk surfaces were carried out in [14] for a system of four cavities, detecting two main flow regimes characterized by two regions: forced convection at small radii and Rayleigh – Bénard convection at medium and large radii.

This paper presents the results of eddy-resolving simulations for turbulent mixed convection in a system of rapidly rotating heated annular cavities located periodically around an inner shaft of a relatively large diameter with axial throughflow of cooling air.

The computations were carried out for conditions close to the experiments in [5] but for a single cavity. We obtained a numerical solution by the ILES method on grids that were much more refined



than those used earlier [7, 8]. We analyzed structures of unsteady flow and temperature fields in the cavities and in the channel supplying the coolant, the evolution of large-scale vortex structures and turbulent fluctuations. Furthermore, we considered the influence of the conditions at the inlet to the cavity on the intensity of local heat transfer from disk surfaces.

### Problem statement and computational aspects

Consider the problem of the flow and heat transfer of air (Prandtl number  $Pr = 0.69$ ) in a system with three rapidly rotating interdisk cavities of the same shape, heated from both disk surfaces and from the periphery, sequentially subjected to axial throughflow of cooling gas (Fig. 1). The system rotates around the  $z$  axis with a constant angular velocity  $\Omega$ .

The computational domain includes three coaxial cavities (denoted by A, B, C by order downstream) and a narrow annular channel interrupted inside each cavity, consisting of an inlet section, two short sections between the cavities and a relatively long outlet section.

The geometry of the cavities and the radial dimension of the axial channel (height) are borrowed from [5], presenting the results of experiments for a single cavity (Table 1).

A constant temperature  $T_{in}$  and a uniform axial velocity profile  $W_{in}$  (without perturbations) are set at the channel inlet (position 1 in Fig. 1), the circumferential component of relative velocity in the inlet section is assumed to be zero. Radial temperature distributions are set on the heated surfaces of disks 6 in each cavity (see Fig. 2, showing the experimental data from [5]; the radial coordinate  $r$  is measured from the central axis), somewhat different for the upstream & downstream disks [5]. Pairs of disks belonging to different cavities are identified as A1-A2, B1-B2, C1-C2 in this study. The temperature is assumed to be constant in the circumferential direction. A linear temperature distribution is set on the surfaces of cylindrical shrouds (position 4 in Fig. 1); it varies slightly between the maximum values on the disks, with  $r/r_0 = 1$ . The inner (2) and outer (3) cylindrical surfaces of the channels are assumed to be thermally insulated. A constant pressure is set at outlet 5 from the channel.

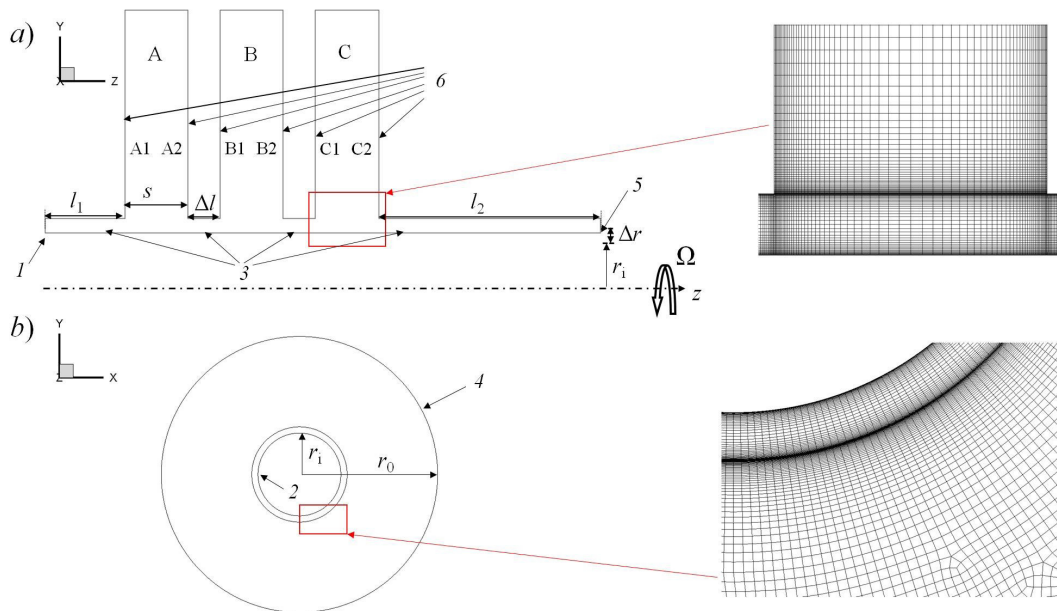


Fig. 1. Schematic illustrating the problem statement for a system of three annular cavities (A, B, C); meridional section of the system (a) and the axial section of one of the disks (b) are shown:

inlet 1; inner and outer pipe surfaces 2 and 3; shroud 4; outlet 5;  
disk surfaces 6 (A1-A2, B1-B2, C1-C2); geometrical parameters are also given.  
Fragments of computational grid for one of the cavities are shown on the right.

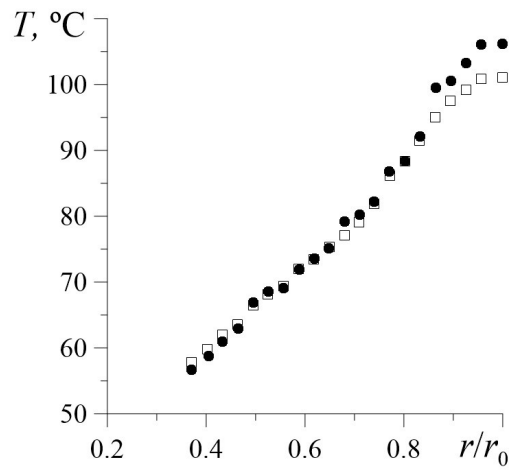


Fig. 2. Experimental radial temperature distributions along the surfaces of the disks [5]: the first (shaded circles) and the second (empty squares) disk downstream.  
Radial coordinate  $r$  is measured from the central axis

Table 1

Computational geometric parameters (see Fig. 1)

Parameter	Notation	Value, m
External cavity radius	$r_0$	0.40
Cavity width	$s$	0.08
Internal radius of annular channel	$r_i$	0.12
Height of annular channel	$\Delta r$	0.018
Length of parts of annular channel:	inlet	0.10
	outlet	0.28
Distance between cavities	$\Delta l$	0.04

Table 2

Remaining computational parameters of the problem

Parameter	Notation	Unit of measurement	Value
Axial velocity of flow	$W_{in}$	m/s	0.95
Angular velocity of system rotation	$\Omega$	rad/s	14.2
Temperature at channel inlet	$T_{in}$	°C	25
Mean temperature at $r = r_0$	$T_0$		104
Temperature factor	$\varepsilon_T$	—	0.27
Reynolds number rotational throughflow	$Re_\Omega$		$2 \cdot 10^5$
	$Re_z$		$2 \cdot 10^4$
Rossby number	Ro		0.56
Prandtl number	Pr		0.69



The numerical solution was obtained in our study for a set of parameters given in Table 2. The data in Table 2 correspond to a set of determining (dimensionless) parameters of the problem, which corresponds to one of the cases known from the literature [5, Case 4].

Traditional hydrodynamic similarity criteria (see Table 2) are defined as follows:

$$\text{Re}_\Omega = \Omega r_0^2 / \nu; \text{Re}_z = 2r_i W_{in} / \nu; \text{Ro} = W_{in} / \Omega r_i,$$

where  $\nu$  is the kinematic viscosity of air (for the inlet temperature).

The temperature factor is estimated by the expression

$$\varepsilon_T = \beta \Delta T,$$

where  $\beta$  is the coefficient of volumetric thermal expansion (also estimated for the inlet temperature),  $\Delta T = T(r = r_0) - T_{in}$ .

Judging from the experimental data shown in Fig. 2, the value  $T_0 = T(r = r_0)$  was taken equal to 104 °C.

The computations were performed in the ANSYS Fluent 19.3 software package. The problem was solved in a relative reference frame rotating at an angular velocity  $\Omega$ , based on the Boussinesq approximation with constant viscosity and thermal conductivity (estimated by the temperature at the inlet to the channel), without taking into account the action of gravity.

We used a computational algorithm based on simultaneous solution of the equations for mass balance and momentum with pressure correction. Spatial discretization of convective terms in the equations was carried out via a QUICK scheme with third-order accuracy. Diffusion terms were approximated by a central-difference scheme with second-order accuracy. The non-iterative fractional step method with second-order accuracy was applied to advance in physical time. The time step was set to  $4 \cdot 10^{-4}$  s, which provided a Courant number of less than unity over the entire computational domain. Representative statistics on the velocity and temperature fields and heat transfer characteristics were accumulated after a transition period (in a time corresponding to approximately 100 revolutions of the cavity system).

The unstructured computational grid whose fragments are shown in Fig. 1 consisted of hexagons, included about 17 million cells, was strongly clustered to all the walls of the computational domain. The grid used was very refined, providing, among other things, the option to reproduce the following phenomena important for satisfactorily predicting the heat transfer process with high accuracy:

- flows in the mixing zones of axial stream with flow in the cavities;
- evolution of multiscale vortex structures in the cavity;
- their interactions with thin quasi-laminar Ekman layers formed near the disk surfaces.

### Computational results and discussion

The details of the three-dimensional vortex pattern of the flow developing in the given system are illustrated in Fig. 3 using the  $Q$ -criterion isosurfaces ( $Q = 400 \text{ s}^{-1}$ ). Apparently, flow with two arms of highly turbulent fluid, and many separate vortical structures in the throughflow zones and at the cavity walls is generated in each of the cavities. The mechanism behind the observed turbulent arms is explained below.

Let us now focus on the particulars of throughflow in the annular channel. Recall that pronounced annular channels are only present in the inlet and outlet sections of the given configuration. Because the conditions of unperturbed uniform flow and a relatively small channel length are adopted for the inlet channel, the boundary layers do not have sufficient time to grow and turbulence does not occur here; consequently, almost uniform throughflow enters the first cavity.



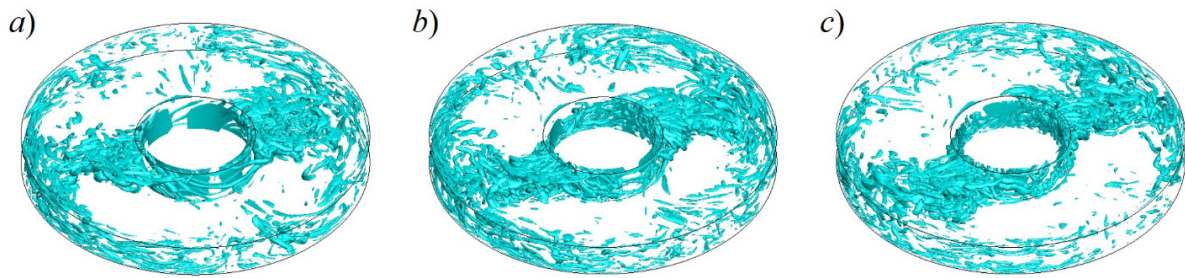


Fig. 3. Visualization of three-dimensional vortex flow through instantaneous  $Q$ -criterion isosurfaces in the cavities A (a), B (b) and C (c) (see Fig. 1);  $Q = 400 \text{ s}^{-1}$

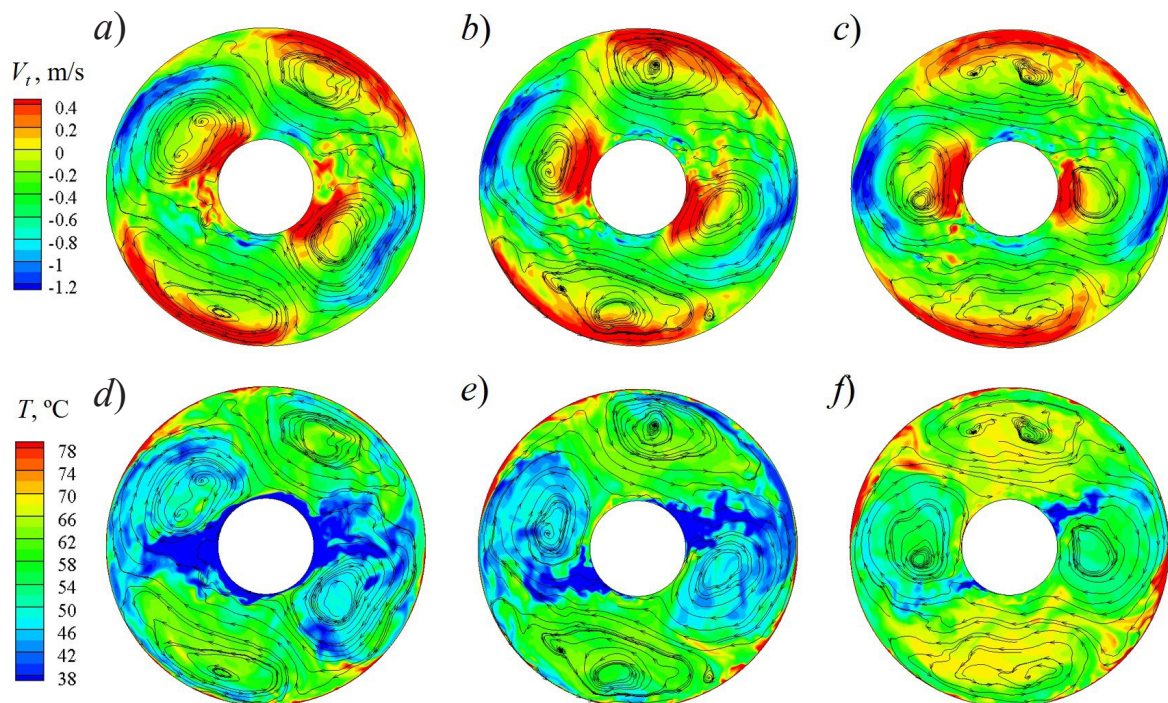


Fig. 4. Instantaneous fields of tangential velocity (a–c) and temperature (d–f) in the central axial section between the disks in the cavities A (a, d), B (b, e), C (c, f) (see Fig. 1)

However, throughflow becomes turbulent already at the outlet from the first cavity, due to its interaction with the fluid in the cavity occurring in the mixing layers. Next, throughflow passes around the sharp edge, entering a short section of the channel between the cavities, and growing considerably turbulent at the inlet to the second (and also the third) cavity.

Fig. 4 shows the instantaneous fields of relative tangential velocity and temperature in the central axial section (with streamlines plotted on them) for all cavities.

Interestingly, the 1990s experiments for cavities with a central axial tube with throughflow of cooling gas [1 – 3] yielded a general picture of fluid circulation typically distinguishing evolving large-scale cyclonic and anticyclonic vortices of the Rayleigh – Bénard type, separated by radial arms of cold gas moving towards the periphery of the region [7, 8, 11 – 13].

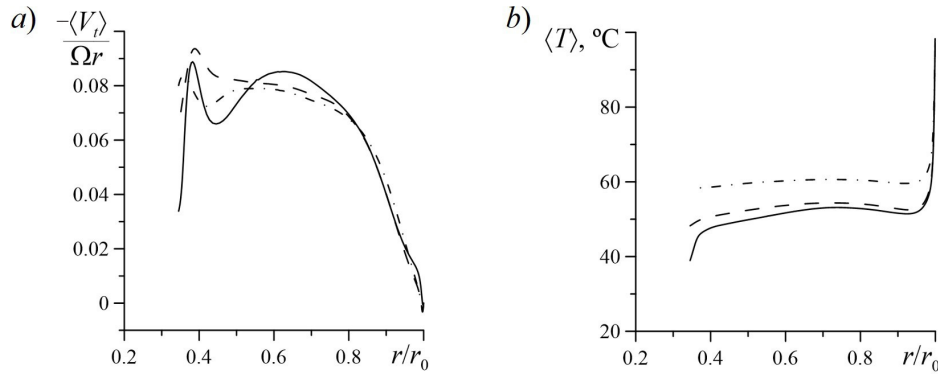


Fig. 5. Computed radial distributions of averaged tangential velocity (a) and temperature (b) in the central axial section between the disks in cavities A (solid line), B (dashed line) and C (dash-dotted line)

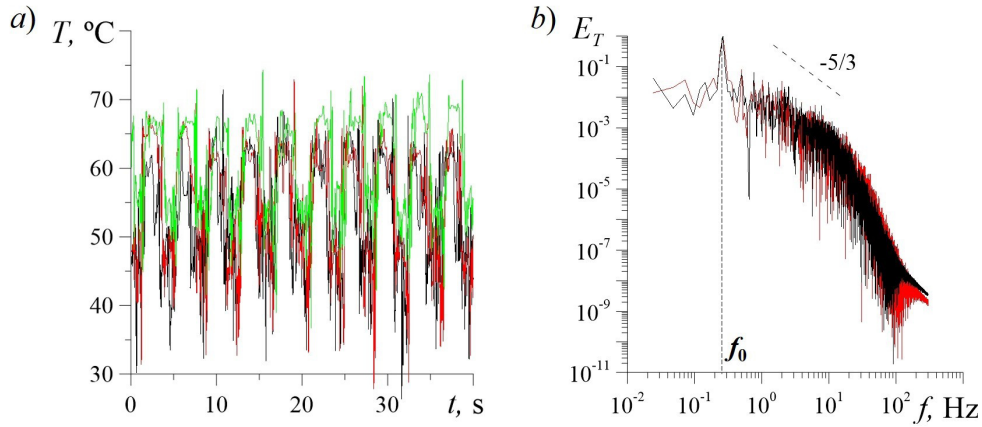


Fig. 6. Temperature fluctuations over time at the monitoring points located in the central sections of the cavities between the disks at a distance  $r = 0.75r_0$  from the axis (a) and the corresponding energy spectrum for points in cavities A and B (b). Computational results are given for cavities A, B and C (black, red and green curves, respectively)

A solution obtained in our computations for an annular cavity included a 'global' anticyclonic vortex surrounding throughflow and a pair of cyclonic vortices pushed to the periphery (Fig. 4). Notably, the turbulent arms of cold gas are located inside the global anticyclonic vortex, producing a pair of local 'internal' anticyclonic vortices. The vortex structure of the flow core is generally preserved over time, with azimuthal motion (precession) in the direction opposite to the direction of rotation.

Fig. 5 shows the radial distributions of tangential velocity and temperature averaged over time and circumferential coordinate for the central section of each of the cavities (angle brackets denote averaging). On average, the flow core noticeably lags behind the translational motion of the system's global rotation (Fig. 5,a). We should note that measurements of circumferential velocity in [15] yielded similar levels of the lag for a related configuration with a single rapidly rotating cavity heated from only one disk; no other experimental data on the rate of lag was found.

The mean temperature of the flow core (Fig. 5,b) varies unevenly along the radius: it is almost constant in most of the cavity, while strong gradients appear near the hot shroud being in contact with regions of relatively cold gas leaking towards it.

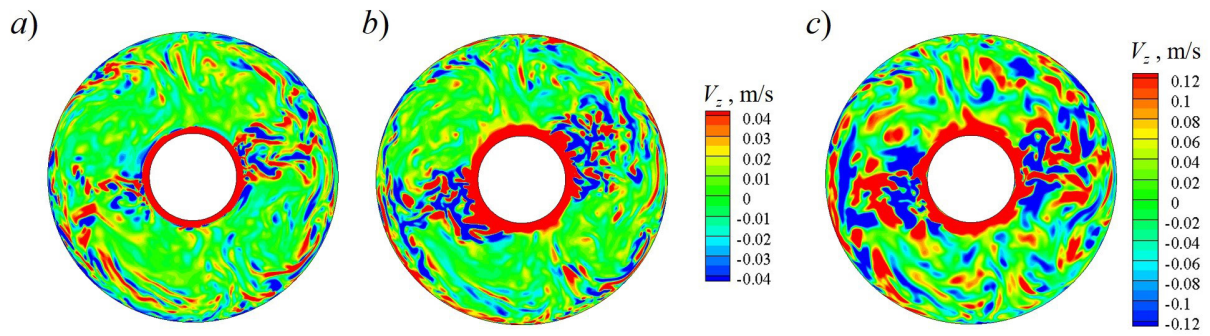


Fig. 7. Instantaneous distributions of axial velocity for the distance of 2.7 mm from the first (a) and the second (b) disk downstream, as well as in the central axial section between the disks in the first cavity (c)

Fig. 6 illustrates the temperature fluctuations over time for all three cavities at the monitoring points located in the central axial sections at a distance  $r = 0.75r_0$  from the axis, as well as the energy spectrum of the fluctuations at the same points for the first and second cavities. The graphs presented confirm that the flow in all cavities has a pronounced turbulent character. The general structure of the fluctuations in the cavities is similar, and their amplitude reaches 0.6 of the temperature difference. The presence of low-frequency fluctuations (with the principal frequency  $f_0 = 0.26$  Hz) reflects the global precession of the flow core discussed above.

Considering small-scale motion, which is largely associated with the phenomena in Ekman layers emerging on disk surfaces, let us first estimate the thickness of these layers. It is well known (see, for example, monograph [3]) that the characteristic thickness  $\delta$  of the 'classical' Ekman layer can be estimated as  $\delta = (\nu/\Omega)0.5$ , and the total thickness of the layer  $\delta_E$  is about  $3\delta$ . The corresponding estimates for the case under consideration give the values  $\delta = 0.9$  mm and  $\delta_E = 2.7$  mm.

Fig. 7 shows the instantaneous axial velocity distributions in the sections located in the first cavity near the disks A1 and A2 at the outer boundaries of the Ekman layers detected by these estimates, as well as in the central axial section between the disks. It can be seen from Fig. 7, a and b that longitudinally oriented vortex structures appear in the Ekman layers, which is definitive proof that hydrodynamic instabilities evolve in these layers. We obtained similar structures in recent computations of free convection in a rapidly rotating closed cavity, introducing near-axis heat sinks to simulate the heat removal effect of throughflow in the initial problem of mixed convection (see [16]). At the moment, we can only assume that given a non-isothermal Ekman layer, these structures act as a trigger giving an impetus to axial motion of the fluid across the cavity in the form of local multidirectional flows with an intensity amounting to tens of percent from the characteristic values of the relative circumferential velocity, providing effective heat transfer between the Ekman layers and the flow core. Further fundamental studies are necessary to gain more insights into this matter.

Fig. 8 shows the temperature fields averaged over time and circumferential direction in the meridional section of the given system of cavities. Evidently, the temperature of throughflow increases considerably as the fluid passes through the cavities. The increases in the mean mass temperature after passing through cavities A, B and C are 13.1, 12.9 and 9.6 °C, respectively. Thus, the values of the temperature factor  $\epsilon_T$  for the three cavities included in the system are different, equal to:  $\epsilon_{T,A} = \epsilon_{T,in} = 0.27$ ;  $\epsilon_{T,B} = 0.21$ ;  $\epsilon_{T,C} = 0.17$  (the characteristic temperature difference  $\Delta T$  and the volumetric thermal expansion  $\beta$  were computed from the mass-averaged temperature at the inlet to the corresponding cavity to obtain estimates for the quantities  $\epsilon_{T,B}$  and  $\epsilon_{T,C}$ ).

Table 3 contains the computational data on the heating power from the disk (quantities  $Q_1$  and  $Q_2$ ) and outer cylindrical ( $Q_3$ ) surfaces of each of the cavities. The last column of Table 3 shows the



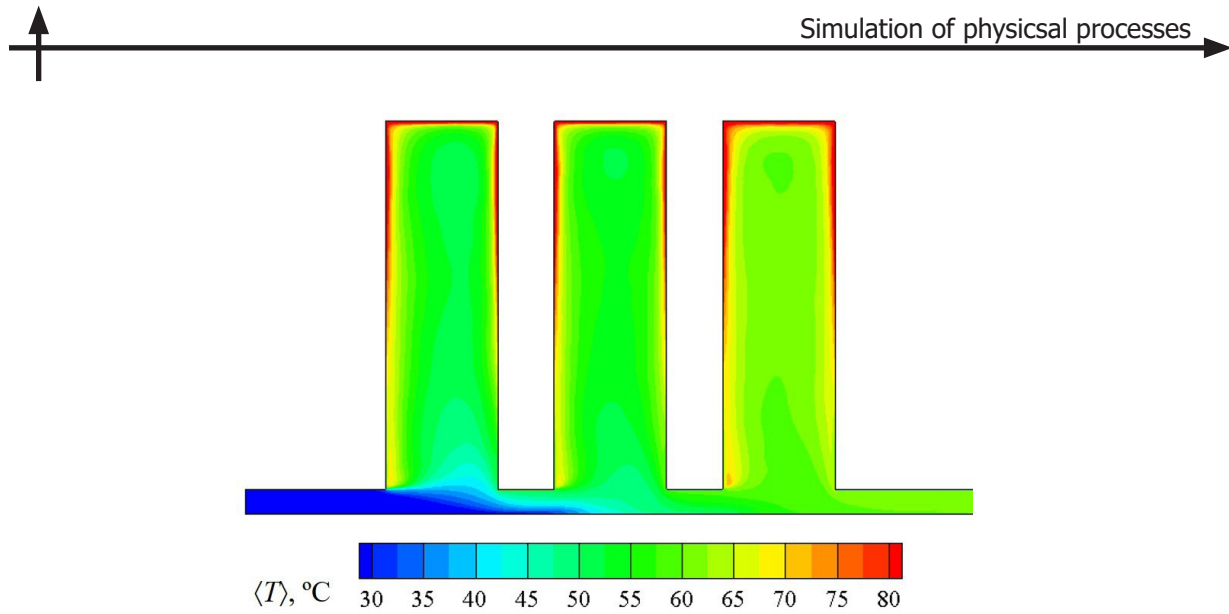


Fig. 8. Computed field of averaged temperature in the meridional section of the system

values of total heat removal  $Q_{\Sigma}$  from the cavity walls. It is noteworthy that the total amount of heat removed per unit time from the walls of the second cavity is close to the value predicted for the first one, while the flow entering the second cavity is already heated (by 13.1 °C) relative to the conditions at the inlet to the first cavity. A likely explanation for this somewhat unexpected result is that throughflow entering the second cavity is highly turbulent, while virtually no turbulent structures are observed at the inlet to the first cavity (under the given boundary conditions). As expected, much less heat is removed from the walls of the third cavity.

Another interesting finding is that integral heat removal from the disks forming the cavity becomes balanced as the flow moves from cavity A to cavity B, and then to cavity C. The difference between  $Q_1$  and  $Q_2$  for the first cavity is 22% (relative to the mean value), and drops to 2.5% for the third cavity.

Turning to the computational results for the local heat transfer intensity, we can observe that the local Nusselt number on the surface of the disks was computed based on the temperature difference between the local value on the wall and the mass-averaged value at the inlet, individual for each cavity.

Fig. 9 shows the computed radial distributions of the local Nusselt number, averaged over time and circumferential coordinate, over the surfaces of all six disks in comparison with the experimental data for a single cavity [5].

The local Nusselt numbers predicted for the first cavity are in fairly satisfactory agreement with the experimental data, especially taking into account their considerable scatter. The greatest discrepancies with the experiment are observed for the first disk downstream, where a section of 'negative' heat transfer is predicted at small radii, which is absent in the experimental data.

Table 3

**Computational data on integral heating power (W) removed from the cavity surfaces**

Cavity	$Q_1$	$Q_2$	$Q_3$	$Q_{\Sigma}$
A	54.4	84.7	79.7	218.8
B	61.4	71.8	81.9	215.1
C	46.3	48.6	65.1	160.0

Notations:  $Q_1$ ,  $Q_2$  are the powers removed from the disk surfaces;  $Q_3$  is the amount of heat removed from the outer cylindrical surface;  $Q_{\Sigma}$  is a value of the total heat removal from the walls of a cavity.

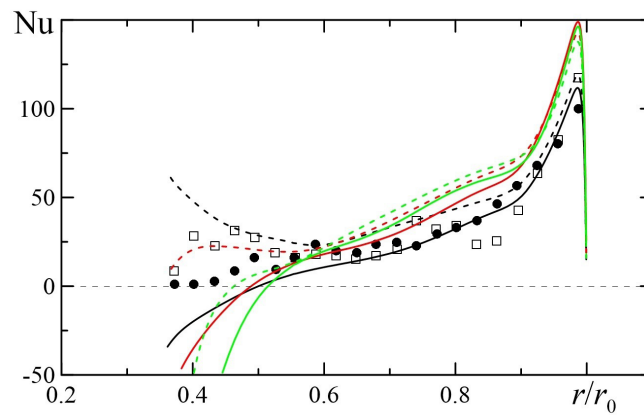


Fig. 9. Comparison of computed radial changes in the local Nusselt number (Nu) on the disk surfaces (lines) with the experimental data from [5] (symbols).

Computational results are shown for cavities A, B and C (black, red and green curves, respectively; solid lines correspond to A1, B1 and C1, dashed lines to A2, B2 and C2). The experimental data are shown similarly to Fig. 2

Moreover, the differences in the conditions at the inlet boundaries of the cavities have a major effect on the computational results. The throughflow entering the second and third cavities is strongly turbulent, contributing to increased normalized heat transfer from the disk surfaces at medium and large radii. A decrease in the temperature factor for the convection developing in the third cavity has a particular pronounced effect on the thickening of the near-surface temperature layer near disk C1 (this is clear from the temperature field shown in Fig. 8) and the appearance of a zone with 'negative' heat transfer with increasing length.

### Conclusion

We have performed numerical simulation of turbulent mixed convection in a multistage system with three rapidly rotating annular cavities heated from disk surfaces and from the periphery and cooled by airflow through a narrow axial annular channel. The computations were based on Implicit Large-Eddy Simulation with a refined computational grid (17 million cells).

The simulation predicted a previously unobserved large-scale structure of the flow in cavities with a global anticyclonic eddy surrounding throughflow and cyclonic vortices localized at large radii. We believe that one of the key reasons why satisfactory agreement with experimental data was obtained was that the evolution of large-scale vortices was described correctly in the computations; small-scale structures responsible for heat transfer between the near-disk layers and the flow core were reproduced simultaneously. Another important finding is that the heat transfer characteristics are highly sensitive to the conditions at the inlet to the cavity.

Ongoing research on this issue is aimed at further developing the eddy-resolving method for computations of this class of flows, which are more complex. This approach is expected to yield reliable and reproducible results. We plan to carry out new computations based on the compressible gas model for a system comprising two or three cavities with varying dynamic and thermal conditions at the cavity inlet, including imposing 'synthetic' turbulence at the inlet.

The study was financed by the Russian Foundation for Basic Research within the framework of Scientific Project "Eddy-resolving modeling of free and mixed convection in rapidly rotating annular cavities" No. 20-08-01090.

The computational results were obtained using the resources of the Supercomputer Center at Peter the Great Polytechnic University ([www.scc.spbstu.ru](http://www.scc.spbstu.ru)).



## REFERENCES

1. **Farthing P.R., Long C.A., Owen J.M., Pincombe J.R.**, Rotating cavity with axial throughflow of cooling air: Flow structure, *J. Turbomach.* 114 (1) (1992) 237–246.
2. **Long C.A.**, Disk heat transfer in a rotating cavity with an axial throughflow of cooling air, *Int. J. Heat Fluid Flow.* 15 (4) (1994) 307–316.
3. **Owen J.M., Rogers R.H.**, Flow and heat transfer in rotating-disk systems, Vol. 2: Rotating cavities, John Wiley & Sons, New York, 1995.
4. **Harmand S., Pelle J., Poncet S., Shevchuk I.V.**, Review of fluid flow and convective heat transfer within rotating disk cavities with impinging jet, *Int. J. Thermal Sciences.* 67 (1) (2013) 1–30.
5. **Bohn D., Deutsch G., Simon B., Burkhardt C.**, Flow visualization in a rotating cavity with axial throughflow, In: *Proc. ASME Turbo Expo 2000*, May 8–11, 2000, Munich, Germany, Paper No. GT2000-280.
6. **Jackson R.W., Luberti D., Tang H., et al.**, Measurement and analysis of buoyancy-induced heat transfer in aero-engine compressor rotor, *J. Eng. Gas Turbines Power.* 143 (6) (2021) 061004.
7. **Bohn D.E., Bouzidi F., Burkhardt C., et al.**, Numerical and experimental investigations of the air flow and heat transfer in rotating cavities, In: *Proc. 9<sup>th</sup> Int. Symp. on Transport Phenomena and Dynamics of Rotating Machinery*, February 10–14, 2002, Honolulu, Hawaii. Paper No. 2002.02.10-14.
8. **Kitanina E.E., Ris V.V., Smirnov E.M., Goryachev V.D.**, Numerical visualization technique for field processing of unsteady natural convection in rotating cavities, In: *Proc. Eurotherm Seminar 71*, October 28–30, 2002, Reims, France (2002) 275–280.
9. **Bohn D., Ren J., Tuemmers C.**, Investigation of the unstable flow structure in a rotating cavity, In: *Proc. ASME Turbo Expo 2006*, 8–11 May, 2006, Barcelona, Spain, Paper No. GT2006-90494.
10. **Smirnov E.M.**, Recent advances in numerical simulation of 3D unsteady convection controlled by buoyancy and rotation, In: *Proc. 12<sup>th</sup> International Heat Transfer Conference*, August 18–23, 2002, Grenoble, France.
11. **Abramov A.G., Zaitsev D.K., Smirnov E.M., Smirnovsky A.A.**, An experience in eddy resolving simulation of mixed convection in a rotating annular cavity with one heated disk and axial throughflow, *J. Phys.: Conf. Ser.* 1683 (2020) 022089.
12. **Abramov A.G., Smirnov S.I., Kitanina E.E., Smirnov E.M.**, Non-stationary vortex structures forming in a heated rapidly rotating annular cavity with axial throughflow of cooling air, In: “Perm Hydrodynamic Scientific Readings”, Proceedings of the 7<sup>th</sup> All-Russian Conference Memorized to Prof. G.Z. Gershuny, E.M. Zhukhovitskiy and D.V. Lyubimov, Perm State University, Perm (2020) 28–37 (in Russian).
13. **Smirnov S.I., Abramov A.G., Kitanina E.E., Smirnov E.M.**, Numerical study of turbulent mixed convection in a rotating inter-disk cavity with axial throughflow of cooling air, *J. Phys.: Conf. Ser.* 1809 (2021) 012013.
14. **Quan Y., Han D., Xu G., et al.**, Convective heat transfer of a rotating multi-stage cavity with axial throughflow, *Int. J. Heat Mass Transfer.* 119 (April) (2018) 117–127.
15. **Owen J.M., Powell J.**, Buoyancy-induced flow in a heated rotating cavity, *J. Eng. Gas Turbines Power.* 128 (1) (2006) 128–134.
16. **Smirnov S.I., Smirnov E.M., Kolesnik E.V.**, Structure of turbulent natural convection in a heated rapidly rotating inter-disk cavity with near-axis heat sinks, *J. Phys.: Conf. Ser.* 1959 (2021) 012045.

*Received 29.06.2021, accepted 26.07.2021.*

## THE AUTHORS

### **SMIRNOV Evgeny M.**

*Peter the Great St. Petersburg Polytechnic University*

29 Politechnicheskaya St., St. Petersburg, 195251, Russian Federation

smirnov\_em@spbstu.ru

### **SMIRNOV Sergei I.**

*Peter the Great St. Petersburg Polytechnic University*

29 Politechnicheskaya St., St. Petersburg, 195251, Russian Federation

sergeysmirnov92@mail.ru

### **ABRAMOV Alexey G.**

*Peter the Great St. Petersburg Polytechnic University*

29 Politechnicheskaya St., St. Petersburg, 195251, Russian Federation

abramov\_ag@spbstu.ru

### **GALAEV Sergey A.**

*Peter the Great St. Petersburg Polytechnic University*

29 Politechnicheskaya St., St. Petersburg, 195251, Russian Federation

galaev@spbstu.ru

## СПИСОК ЛИТЕРАТУРЫ

1. **Farthing P.R., Long C.A., Owen J.M., Pincombe J.R.** Rotating cavity with axial throughflow of cooling air: Flow structure // *J. Turbomach.* 1992. Vol. 114. No. 1. Pp. 237–246.
2. **Long C.A.** Disk heat transfer in a rotating cavity with an axial throughflow of cooling air // *Int. J. Heat Fluid Flow.* 1994. Vol. 15. No. 4. Pp. 307–316.
3. **Owen J.M., Rogers R.H.** Flow and heat transfer in rotating-disk systems. Vol. 2: Rotating cavities. New York: John Wiley & Sons, 1995. 295 p.
4. **Harmand S., Pelle J., Poncet S., Shevchuk I.V.** Review of fluid flow and convective heat transfer within rotating disk cavities with impinging jet // *Int. J. Thermal Sciences.* 2013. Vol. 67. No. 1. Pp. 1–30.
5. **Bohn D., Deutsch G., Simon B., Burkhardt C.** Flow visualization in a rotating cavity with axial throughflow // *Proc. ASME Turbo Expo 2000*, May 8–11, 2000, Munich, Germany. Paper No. GT2000-280. 8 p.
6. **Jackson R.W., Luberti D., Tang H., Pountney O.J., Scobie J.A., Sangam C.M., Owen J.M., Lock G.D.** Measurement and analysis of buoyancy-induced heat transfer in aero-engine compressor rotor // *J. Eng. Gas Turbines Power.* 2021. Vol. 143. No. 6. P. 061004.
7. **Bohn D.E., Bouzidi F., Burkhardt C., Kitanina E.E., Ris V.V., Smirnov E.M., Wolff M.W.** Numerical and experimental investigations of the air flow and heat transfer in rotating cavities // *Proc. 9<sup>th</sup> Int. Symp. on Transport Phenomena and Dynamics of Rotating Machinery*; February 10–14, 2002, Honolulu, Hawaii. Paper No. 2002.02.10-14. 8 p.
8. **Kitanina E.E., Ris V.V., Smirnov E.M., Goryachev V.D.** Numerical visualization technique for field processing of unsteady natural convection in rotating cavities // *Proc. Eurotherm Seminar 71*; October 28–30, 2002, Reims, France. Pp. 275–280.
9. **Bohn D., Ren J., Tuemmers C.** Investigation of the unstable flow structure in a rotating cavity // *Proc. ASME Turbo Expo 2006*; 8–11 May, 2006, Barcelona, Spain. Paper No. GT2006-90494. 10 p.





10. **Smirnov E.M.** Recent advances in numerical simulation of 3D unsteady convection controlled by buoyancy and rotation // Proc. 12<sup>th</sup> International Heat Transfer Conference; August 18–23, 2002, Grenoble, France. 12 p.
11. **Abramov A.G., Zaitsev D.K., Smirnov E.M., Smirnovsky A.A.** An experience in eddy resolving simulation of mixed convection in a rotating annular cavity with one heated disk and axial throughflow // J. Phys.: Conf. Ser. 2020. Vol. 1683. P. 022089.
12. **Абрамов А.Г., Смирнов С.И., Китанина Е.Э., Смирнов Е.М.** Нестационарные вихревые структуры, формирующиеся в нагреваемой быстровращающейся кольцевой полости с транзитным осевым потоком охлаждающего воздуха // Пермские гидродинамические научные чтения. Материалы VII Всероссийской конференции с международным участием, посвященной памяти профессоров Г.З. Гершуни, Е.М. Жуховицкого и Д.В. Любимова. Пермь: Пермский государственный национальный исследовательский университет, 2020. С. 28–37.
13. **Smirnov S.I., Abramov A.G., Kitanina E.E., Smirnov E.M.** Numerical study of turbulent mixed convection in a rotating inter-disk cavity with axial throughflow of cooling air // J. Phys.: Conf. Ser. 2021. Vol. 1809. P. 012013.
14. **Quan Y., Han D., Xu G., Wen J., Luo X.** Convective heat transfer of a rotating multi-stage cavity with axial throughflow // Int. J. Heat Mass Transf. 2018. Vol. 119. April. Pp. 117–127.
15. **Owen J.M., Powell J.** Buoyancy-induced flow in a heated rotating cavity // J. Eng. Gas Turbines Power. 2006. Vol. 128. No. 1. Pp. 128–134.
16. **Smirnov S.I., Smirnov E.M., Kolesnik E.V.** Structure of turbulent natural convection in a heated rapidly rotating inter-disk cavity with near-axis heat sinks // J. Phys.: Conf. Ser. 2021. Vol. 1959. P. 012045.

*Статья поступила в редакцию 29.06.2021, принята к публикации 26.07.2021.*

## СВЕДЕНИЯ ОБ АВТОРАХ

**СМИРНОВ Евгений Михайлович** — доктор физико-математических наук, профессор Высшей школы прикладной математики и вычислительной физики, главный научный сотрудник Научно-исследовательской лаборатории гидроаэродинамики Санкт-Петербургского политехнического университета Петра Великого, Санкт-Петербург, Российская Федерация.

195251, Российская Федерация, г. Санкт-Петербург, Политехническая ул., 29  
smirnov\_em@spbstu.ru

**СМИРНОВ Сергей Игоревич** — кандидат физико-математических наук, инженер Научно-образовательного центра «Компьютерные технологии в аэродинамике и теплотехнике» Санкт-Петербургского политехнического университета Петра Великого, Санкт-Петербург, Российская Федерация.

195251, Российская Федерация, г. Санкт-Петербург, Политехническая ул., 29  
sergeysmirnov92@mail.ru

**АБРАМОВ Алексей Геннадьевич** — кандидат физико-математических наук, доцент Высшей школы прикладной математики и вычислительной физики Санкт-Петербургского политехнического университета Петра Великого, Санкт-Петербург, Российская Федерация.

195251, Российская Федерация, г. Санкт-Петербург, Политехническая ул., 29  
abramov\_ag@spbstu.ru

**ГАЛАЕВ Сергей Александрович** — кандидат технических наук, доцент Высшей школы прикладной математики и вычислительной физики Санкт-Петербургского политехнического университета Петра Великого, Санкт-Петербург, Российская Федерация.

195251, Российская Федерация, г. Санкт-Петербург, Политехническая ул., 29  
galaev@spbstu.ru